

# Polycyclic $\pi$ -Electron System with Boron at Its Center

Shohei Saito,\* Kyohei Matsuo, and Shigehiro Yamaguchi\*

Department of Chemistry, Graduate School of Science, Nagoya University and JST-CREST, Furo, Chikusa, Nagoya 464-8602, Japan

**S** Supporting Information

**ABSTRACT:** We disclose a new planarized triarylborane in which the tri-coordinated boron atom is embedded in a fully fused polycyclic  $\pi$ -conjugated skeleton. The compound shows high stability toward oxygen, water, and silica gel, despite the absence of steric protection around the B atom. Reflecting the electron-donating character of the  $\pi$ -skeleton and the electron-accepting character of the B atom, this compound shows broad absorption bands that cover the entire visible region and a fluorescence in the visible/near-IR region. In addition, this compound shows dramatic property changes upon formation of a tetra-coordinated borate, such as thermochromic behavior in the presence of pyridine.

Boron-containing  $\pi$ -conjugated materials have been extensively studied because of their intriguing electronic features, including strong electron-accepting character and strong Lewis acidity, which make promising themselves for use as emissive organic solid materials, two-photon absorbing materials, electron-transporting materials, and chemosensors for anions.<sup>1</sup> In designing new B-containing  $\pi$ -systems, one of the central issues to overcome is the intrinsic instability against moisture and oxygen. Two approaches have been generally adopted. One is the introduction of bulky substituents to sterically protect the Lewis acidic B atom.<sup>2</sup> However, bulky substituents prevent intermolecular interactions in the solid state, which is disadvantageous for gaining high carrier transporting properties. The other approach is the replacement of B–C bonds with B–N or B–O bonds, which has yielded a number of fascinating  $\pi$ -systems with reasonable stabilities.<sup>3</sup> However, interaction between the lone-pair electrons of the heteroatom and the vacant p orbital of the B atom diminishes the inherent virtue of the boron compounds, i.e., the electron-accepting character and the Lewis acidity.

We recently disclosed the structural constraint as an alternative strategy for stabilizing organoboron compounds. We synthesized a triphenylborane **1** ( $\pi$  = benzene in Figure 1a), rigidly fixed in a planar fashion with three methylene tethers, and demonstrated that this compound showed a high stability toward water, oxygen, amines, and silica gel.<sup>4</sup> In addition, the completely planarized skeleton effectively spreads the  $\pi$ -conjugation among the three phenyl groups through the B atom, leading to some intriguing properties. However, as the  $sp^3$  carbon bridges do not expand the  $\pi$ -electron delocalization, **1** showed only an absorption band in the UV region. Moreover, the dimethyl groups on the bridging methylene moieties in **1** still prevented intermolecular contact in the crystalline state.

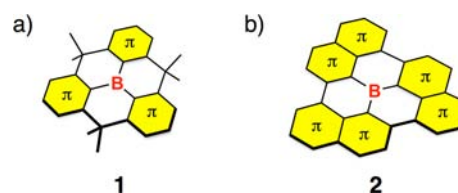


**Figure 1.** (a) Methylene-bridged planarized triarylborane **1** and (b) fully  $\pi$ -conjugated planarized triarylborane **2**.

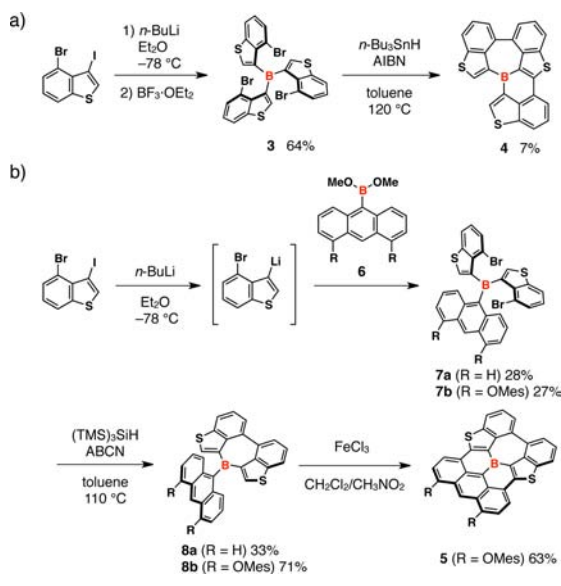
To compensate for these drawbacks and produce a more sophisticated B-containing  $\pi$ -system, we have now synthesized a new planarized triarylborane **2**, in which the three aryl groups on the B atom are fully conjugated to one another (Figure 1b). This compound can be regarded as a model of a B-doped graphene fragment. We reveal that the high planarity indeed allows this triarylborane skeleton to form a face-to-face  $\pi$ -stacked structure. Moreover, this polycyclic  $\pi$ -skeleton shows interesting photophysical properties due to the B atom, such as long-wavelength absorption and emission as well as a thermoresponsive color change in the presence of a Lewis base.

Our initial target molecule for a peripherally  $\pi$ -conjugated triarylborane was fully planarized tris(benzo[*b*]thienyl)borane **2** ( $\pi$  = benzothiophene). We envisioned that this skeleton could be constructed by three-fold intramolecular coupling from tris(4-bromo-3-benzothiophenyl)borane **3** (Scheme 1a). The precursor **3** was obtained in 64% yield from 4-bromo-3-iodobenzothiophene. A crystal structure analysis confirmed that **3** has a propeller-like structure suitable for  $C_3$ -symmetric three-fold cyclization (Supporting Information (SI)). We first attempted intramolecular Pd-catalyzed C–H arylation under various conditions with bases such as  $K_2CO_3$  and DBU.<sup>5</sup> However, these reactions resulted in the undesired B–C bond cleavage. Therefore, an intramolecular radical cyclization<sup>6</sup> using  $n$ - $Bu_3SnH$  with AIBN as initiator in toluene at 120 °C was next conducted. Although this reaction did not produce the target product, we were able to isolate a doubly cyclized compound **4** in 7% yield. This result suggested some important implications. Thus, the B–C bonds of the triarylborane can remain intact under the radical reaction conditions. The homocoupling of the two C–Br bonds precedes the cross-coupling between the C–Br and C–H bonds, resulting in the formation of the B-containing seven-membered ring. Moreover, the doubly cyclized product **4** is barely stable enough to isolate by column chromatography on silica gel. These insights prompted us to synthesize the next target **5**, which has an anthracene skeleton in place of one of the benzothiophene skeletons (Scheme 1b).

Received: April 21, 2012

Published: May 17, 2012

## Scheme 1. Synthesis of Planarized Triarylboranes



We envisioned that the incorporation of the anthracene unit would allow us to employ the oxidative cyclization for constructing a fully ring-fused  $\pi$ -skeleton in the final step.<sup>7</sup>

For the synthesis of **5**, anthrylbis(bromobenzothiényl)boranes **7** were prepared as the key precursor from 4-bromo-3-iodobenzothiophene and anthryldimethoxyboranes **6**. Radical-promoted intramolecular homocoupling from **7** was then conducted using  $(\text{TMS})_3\text{SiH}$  with 1,1'-azobis(cyclohexanecarbonitrile) (ABCN) as an initiator to give the cyclized products **8a** and **8b** in 33% and 71% yields, respectively. Crystal structural analysis of **8a** revealed the perpendicular arrangement of the anthryl group to the di(benzothiényl)borane plane (SI). When we attempted the oxidative cyclization of **8a** using  $\text{FeCl}_3$ , only a black complex mixture was obtained. This is probably due to the low selectivity of the intramolecular cyclization over the intermolecular reactions.<sup>8</sup> The poor solubility of the highly planar product may also be a problem. To solve these problems, we decided to introduce bulky mesityloxy (-OMe) groups to the 4,5-positions of the anthracene unit, which should suppress the intermolecular reaction as well as the aggregation of the product and, at the same time, increase the reactivity at the 1,8-positions, resulting in selective intramolecular cyclization.<sup>9</sup> In fact, the reaction of **8b** (R = OMe) with  $\text{FeCl}_3$  successfully produced **5** in 63% yield as a deep purple solid. Notably, product **5** as well as all the precursors **6**–**8** are stable enough to handle in the air and isolate by silica gel column chromatography without any special precautions. Thus, a glovebox system is unnecessary for the entire synthetic process. The high stability of **5** despite the absence of steric protection is attributable to the effect of the structural constraint. The rigid and cyclic  $\pi$ -skeleton around the B atom retards a decomposition process that proceeds through the reaction with Lewis bases, because a tetra-coordinated intermediate is destabilized and/or a C–B bond cleavage from the intermediate is prevented by the chelating effect.<sup>4</sup> The high thermal stability of **5** is also demonstrated by thermogravimetric analysis: the decomposition temperature for a 5% weight loss was  $424^\circ\text{C}$ .

Single crystals of **5** suitable for X-ray diffraction analysis were obtained by vapor diffusion of octane into a toluene solution of the compound. The crystal structure confirmed that the tri-

coordinated B atom is embedded in the center of the 10-ring-fused  $\pi$ -skeleton in the form of a borepin<sup>2d,e</sup>-like seven-membered ring (Figure 2a). The high planarity is confirmed by

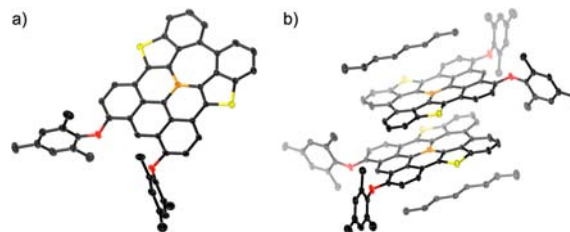


**Figure 2.** (a) Crystal structure of **5** (50% probability for thermal ellipsoids) and (b)  $\pi$ -stacked dimer in the crystal packing.

the small mean plane deviation of  $0.15\text{ \AA}$  as well as the small dihedral angles between the anthracene and benzothiophene planes ( $1.5^\circ$  and  $4.0^\circ$ , SI). The central B atom is confined to the planar  $\pi$ -skeleton with the sum of the three C–B–C angles of  $360.0^\circ$ . The B–C<sub>thienyl</sub> ( $1.508(2)$  and  $1.513(2)\text{ \AA}$ ) and B–C<sub>anthryl</sub> ( $1.539(2)\text{ \AA}$ ) bond lengths are much shorter than those of triphenylborane ( $1.57$ – $1.59\text{ \AA}$ )<sup>10</sup> and trimesitylborane ( $1.57$ – $1.58\text{ \AA}$ ),<sup>11</sup> and comparable to those of the methylene-bridged triphenylborane **1** ( $1.52\text{ \AA}$ ).<sup>4</sup> Importantly, in the crystal packing, **5** forms  $\pi$ -stacked dimers with a mean plane distance of  $3.53\text{ \AA}$  (Figure 2b). This is an unprecedented structure for a triarylborane-based  $\pi$ -system. The bulky Mes groups are arranged almost perpendicular to the  $\pi$ -system, and octanes are located above and below the  $\pi$ -stacked dimer.

The planarized borane **5** showed interesting photophysical properties (see Figure 3a). Its toluene solution exhibited a purple color and showed broad absorption bands that covered the entire visible region of  $400$ – $730\text{ nm}$ , with maximum wavelengths ( $\lambda_{\text{abs}}$ ) of  $527$ ,  $563$ ,  $620$ , and  $668\text{ nm}$ . These

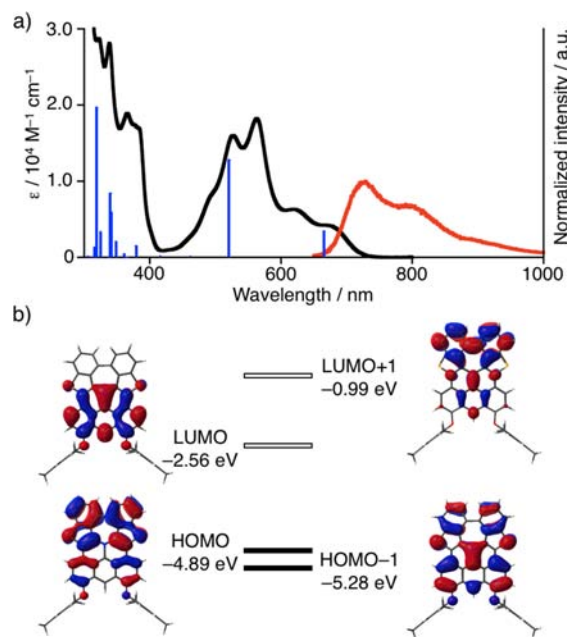


**Figure 3.** (a) UV/vis absorption (black line) and vis/near-IR fluorescence (red line) spectra of **5** in toluene along with the oscillator strengths (blue bars) obtained by the TD-DFT (B3LYP/6-31G\*) calculation. (b) Kohn-Sham molecular orbitals of **5** calculated at the B3LYP/6-31G\* level.

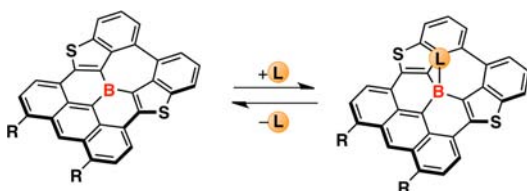
absorption maxima are significantly longer than the longest  $\lambda_{\text{abs}}$  of **1** (320(sh) nm), demonstrating the impact of the peripheral expansion of  $\pi$ -conjugation. Moreover, this compound showed fluorescence in the vis/near-IR region with maximum wavelength ( $\lambda_{\text{em}}$ ) of 729 nm. Since most triarylboranes fluoresce only in the visible region,<sup>12</sup> this near-IR fluorescence is a unique property for the present B  $\pi$ -system, although the quantum yield is low, 0.016. These absorption and emission bands showed negligible or only subtle solvent effects (SI).

To elucidate the photophysical properties, a DFT (B3LYP/6-31G\*) calculation was conducted for **5** (Figure 3b).<sup>13</sup> This compound has both a rather high-lying HOMO and a low-lying LUMO. The HOMO is mainly delocalized over the “oxyphenylbenzothiophene dimer” moiety, while the HOMO–1 is delocalized over the entire  $\pi$ -skeleton with a contribution from the p orbital of the B atom. On the other hand, the LUMO is mostly localized on the borylanthracene moiety with a contribution from the p– $\pi^*$  interaction.<sup>1</sup> The LUMO level of **5** (–2.56 eV) is much lower than that of **1** (–1.56 eV). The TD-DFT calculation at the same level of theory suggested that the broad visible absorption bands consist of two transitions accompanied by vibronic structures, which are assignable to the HOMO→LUMO and the HOMO–1→LUMO transitions. Their calculated transition energies are 1.86 eV (666 nm) and 2.38 eV (522 nm), respectively. The smaller oscillator strength for the longer-wavelength absorption band was also reproduced by the TD-DFT calculation (SI). This calculation demonstrated that the key factor for realizing absorption and emission at significantly long wavelengths is to incorporate the electron-accepting tri-coordinated B atom into the highly electron-donating polycyclic  $\pi$ -skeleton.

To experimentally gain insights into the electronic structure, cyclic voltammetry was conducted in THF using *n*-Bu<sub>4</sub>NPF<sub>6</sub> as the supporting electrolyte (SI). Notably, **5** showed reversible redox waves both for oxidation and reduction, demonstrating that the generated radical cation and radical anion are stable under the measurement conditions. The first half-reduction and oxidation potentials ( $E_{1/2}$ ) were –1.37 and 0.60 V (vs Fc/Fc<sup>+</sup>), respectively.

The most important structural feature of **5** is that the tri-coordinated B atom is surrounded by a rigid and planar  $\pi$ -skeleton. We are interested in whether this B compound still maintains Lewis acidity and forms a complex with a Lewis base. To study this issue, we treated **5** with several Lewis bases (Scheme 2).<sup>14</sup> Upon the addition of *n*-Bu<sub>4</sub>NF or *n*-Bu<sub>4</sub>NCN to

#### Scheme 2. Interconversion between **5** and the Corresponding Borate by Reaction with a Lewis Base



a THF solution of **5**, the color of the solution dramatically changed from purple to yellow. The UV/vis spectra showed that as the amount of the base increased, the absorption bands of **5** around 670 and 560 nm disappeared and a new band at 478 nm appeared, which is assignable to a tetra-coordinated B species (SI). In line with this change, the <sup>11</sup>B NMR spectrum of **5** was converted from a broad peak at 39.5 ppm to a sharp one

at 1.6 ppm in CDCl<sub>3</sub> by the addition of an excess amount of *n*-Bu<sub>4</sub>NF. The binding constant (*K*) of **5** with a fluoride ion in THF was determined by UV/vis titration to be  $1.3 \times 10^5 \text{ M}^{-1}$ , which is slightly lower than those of the methylene-bridged triphenylborane **1** ( $7.0 \times 10^5 \text{ M}^{-1}$ )<sup>4</sup> and trimesitylborane ( $3.3 \times 10^5 \text{ M}^{-1}$ ).<sup>14a</sup> This comparison demonstrates that **5** keeps its Lewis acidity, but the degree is diminished by the structural restriction. Interestingly, **5** has a much lower-lying LUMO than **1** (*vide supra*). Nevertheless, the Lewis acidity of **5** is weaker than that of **1**, demonstrating the impact of the more rigid structure of **5**.

When **5** was treated with a weaker Lewis base, pyridine, an interesting thermochromism was observed: the color of a pyridine/THF (1:3) solution of **5** changed dramatically from purple at a higher temperature to yellow at a lower temperature (see Figure 4a). We quantitatively analyzed this phenomenon

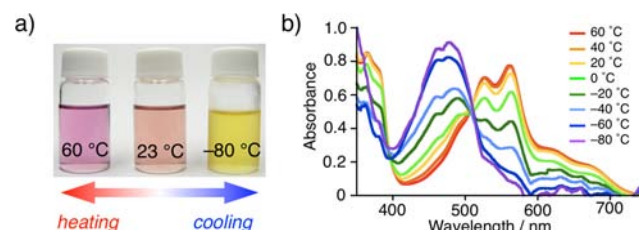


**Figure 4.** (a) Thermochromism of a 1:3 pyridine/THF solution of **5**. (b) Absorption spectral change of **5** ( $4.66 \times 10^{-5} \text{ M}$ ) in a 1:15 pyridine/THF mixed solvent.

by UV/vis titration as well as variable-temperature UV/vis absorption spectra. The binding constant of **5** with pyridine in THF had the very low value of  $K = 0.35 \text{ M}^{-1}$  at 23 °C. As the temperature decreased from 60 to –80 °C, the absorption bands at 563 and 668 nm decreased in intensity, and the intensity of the bands at 485 and 461 nm increased, with isosbestic points at 508 and 397 nm, as shown in Figure 4b. Based on these results, the parameters for the equilibrium between **5** and the **5**·pyridine complex were estimated to be  $\Delta H = -21.3 \text{ kJ mol}^{-1}$  and  $\Delta S = -76.2 \text{ J K}^{-1} \text{ mol}^{-1}$ . As a result, the Gibbs energy change ( $\Delta G$ ) for this equilibrium becomes negative at low temperature but positive at high temperature, and thereby this system shows thermochromism. The weak Lewis acidity of **5** is responsible for this thermoresponsive behavior.

Finally, the structure of the tetra-coordinated **5**·F<sup>–</sup> was confirmed by X-ray crystallography as a K<sup>+</sup>([2.2.2]cryptand) salt (Figure 5):<sup>15</sup> the polycyclic  $\pi$ -skeleton still has high planarity, and only the central B atom deviates from the  $\pi$ -plane. The dihedral angles between the anthracene and

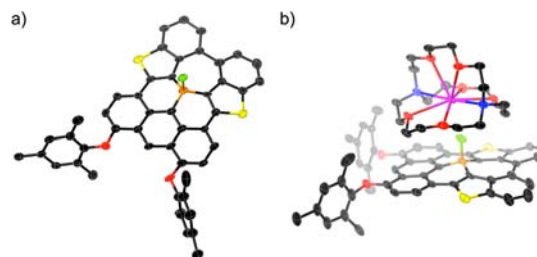


**Figure 5.** X-ray crystal structure of **5**·F<sup>–</sup>[K(cryptand)]<sup>+</sup> (50% probability for thermal ellipsoids). (a) Top view, in which [K(cryptand)]<sup>+</sup> was omitted for clarity, and (b) side view.

benzothiophene units are  $3.0^\circ$  and  $13.4^\circ$ , and that between the two benzothiophene units is  $16.3^\circ$ . The B–C bond lengths (1.579(9), 1.584(8), and 1.596(9) Å) are longer than those of **5** but still much shorter than those of standard triarylfluoroborates (1.62–1.68 Å).<sup>16</sup> The sum of the three C–B–C angles of  $337.1^\circ$  in  $5\cdot\text{F}^-$  corresponds to the small tetrahedral character of 73%,<sup>17</sup> indicating that the structural constraint significantly restrains the deformation to the tetrahedral structure. This fact should be relevant to the weak Lewis acidity.

In summary, we have succeeded in the synthesis of a new planarized triarylborane, in which tri-coordinated B is embedded in the electron-donating polycyclic  $\pi$ -skeleton. The compound shows remarkable chemical and thermal stabilities and can be handled without special care. Different from the previous methylene-bridged planar triphenylborane, the highly planar skeleton indeed forms a face-to-face  $\pi$ -stacked structure. In light of this structural feature as well as its interesting electronic features with the narrow HOMO–LUMO gap, this expanded  $\pi$ -conjugated borane should have significant potential for optoelectronic applications. The interconversion between the tri-coordinated borane and the tetra-coordinated borate is the other fascinating feature of this boron-centered  $\pi$ -system, which results in dramatic property changes, such as thermochromic behavior in the presence of pyridine. Further studies on the application of this boron  $\pi$ -system as well as the synthesis of more sophisticated planar boron-centered  $\pi$ -skeletons are currently underway in our laboratory.

## ■ ASSOCIATED CONTENT

### Supporting Information

Experimental procedures; X-ray crystal structures (PDF, CIF) of **5** (CCDC-873940),  $5\cdot\text{F}^-[\text{K}(\text{cryptand})]^+$  (CCDC-873941), **3**, and **8a**; theoretical calculations; cyclic voltammogram; titration experiments; and complete ref 13. This material is available free of charge via the Internet at <http://pubs.acs.org>.

## ■ AUTHOR INFORMATION

### Corresponding Author

s\_saito@chem.nagoya-u.ac.jp; yamaguchi@chem.nagoya-u.ac.jp

### Notes

The authors declare no competing financial interest.

## ■ ACKNOWLEDGMENTS

This work was supported by a Grant-in-Aid (No. 19675001) from the Ministry of Education, Culture, Sports, Science, and Technology, Japan and CREST, JST. S.S. is grateful to the Japan Society for the Promotion of Science for a Grant-in-Aid for Research Activity Start-up. The authors thank Prof. A. Osuka, Dr. N. Aratani, and Dr. T. Tanaka (Kyoto University) for measurement of variable-temperature UV/vis absorption spectra.

## ■ REFERENCES

(1) Reviews: (a) Entwistle, C. D.; Marder, T. B. *Angew. Chem., Int. Ed.* **2002**, *41*, 2927. (b) Entwistle, C. D.; Marder, T. B. *Chem. Mater.* **2004**, *16*, 4574. (c) Jäkle, F. *Coord. Chem. Rev.* **2006**, *250*, 1107. (d) Yamaguchi, S.; Wakamiya, A. *Pure Appl. Chem.* **2006**, *78*, 1413. (e) Bosdet, M. J. D.; Piers, W. E. *Can. J. Chem.* **2008**, *86*, 8. (f) Wade, C. R.; Broomsgrove, A. E. J.; Aldridge, S.; Gabbai, F. P. *Chem. Rev.* **2010**, *110*, 3958. (g) Jäkle, F. *Chem. Rev.* **2010**, *110*, 3985. (h) Hudson, Z. M.; Wang, S. *Dalton Trans.* **2011**, *40*, 7805.

(2) (a) Yamaguchi, S.; Shirasaka, T.; Akiyama, S.; Tamao, K. *J. Am. Chem. Soc.* **2002**, *124*, 8816. (b) Yuan, Z.; Entwistle, C. D.; Collings, N. J.; Albesa-Jové, D.; Batsanov, A. S.; Howard, J. A. K.; Taylor, N. J.; Kaiser, H. M.; Kaufmann, D. E.; Poon, S.-Y.; Wong, W.-Y.; Jardin, C.; Fathallah, S.; Boucekkin, A.; Halet, J.-F.; Marder, T. B. *Chem. Eur. J.* **2006**, *12*, 2758. (c) Wakamiya, A.; Mishima, K.; Ekawa, K.; Yamaguchi, S. *Chem. Commun.* **2008**, 579. (d) Mercier, L. G.; Piers, W. E.; Parvez, M. *Angew. Chem., Int. Ed.* **2009**, *48*, 6108. (e) Caruso, A., Jr.; Siegler, M. A.; Tovar, J. D. *Angew. Chem., Int. Ed.* **2010**, *49*, 4213.

(3) (a) Bosdet, M. J. D.; Sorensen, T. S.; Piers, W. E.; Parvez, M. *Angew. Chem., Int. Ed.* **2007**, *46*, 4940. (b) Brothers, P. J. *Chem. Commun.* **2008**, 2090. (c) Marwitz, A. J. V.; Matus, M. H.; Zakharov, L. N.; Dixon, D. A.; Liu, S.-Y. *Angew. Chem., Int. Ed.* **2009**, *48*, 973. (d) Tsurumaki, E.; Hayashi, S.; Tham, F. S.; Reed, C. A.; Osuka, A. *J. Am. Chem. Soc.* **2011**, *133*, 11956. (e) Hatakeyama, T.; Hashimoto, S.; Seki, S.; Nakamura, M. *J. Am. Chem. Soc.* **2011**, *133*, 18614.

(4) Zhou, Z.; Wakamiya, A.; Kushida, T.; Yamaguchi, S. *J. Am. Chem. Soc.* **2012**, *134*, 4529.

(5) (a) Reisch, H. A.; Bratcher, M. S.; Scott, L. T. *Org. Lett.* **2000**, *2*, 1427. (b) Alberico, D.; Scott, M. E.; Lautens, M. *Chem. Rev.* **2007**, *107*, 174. (c) Pascual, S.; Mendoza, P.; Echavarren, A. M. *Org. Biomol. Chem.* **2007**, *5*, 2727.

(6) (a) Harrowven, D. C.; Guy, I. L.; Nanson, L. *Angew. Chem., Int. Ed.* **2006**, *45*, 2242. (b) Rajca, A.; Miyasaka, M.; Xiao, S.; Boratyński, P. J.; Pink, M.; Rajca, S. *J. Org. Chem.* **2009**, *74*, 9105. (c) Castillo, R. R.; Burgos, C.; Vaqueromgrt, J. J.; Alvarez-Builla, J. *Eur. J. Org. Chem.* **2011**, 619.

(7) (a) Watson, M.; Fechtenkötter, A.; Müllen, K. *Chem. Rev.* **2001**, *101*, 1267. (b) Wu, J.; Pisula, W.; Müllen, K. *Chem. Rev.* **2007**, *107*, 718.

(8) King, B. T.; Kroulík, J.; Robertson, C. R.; Rempala, P.; Hilton, C. L.; Korinek, J. D.; Gortari, L. M. *J. Org. Chem.* **2007**, *72*, 2279.

(9) (a) Davis, N. K. S.; Thompson, A. L.; Anderson, H. L. *Org. Lett.* **2010**, *12*, 2124. (b) Davis, N. K. S.; Thompson, A. L.; Anderson, H. L. *J. Am. Chem. Soc.* **2011**, *133*, 30. (c) Zeng, L.; Jiao, C.; Huang, X.; Huang, K.-W.; Chin, W.-S.; Wu, J. *Org. Lett.* **2011**, *13*, 6026.

(10) Zettler, F.; Hausen, H. D.; Hess, H. *J. Organomet. Chem.* **1974**, *72*, 157.

(11) (a) Blount, J. F.; Finocchiaro, P.; Gust, D.; Mislow, K. *J. Am. Chem. Soc.* **1973**, *95*, 7019. (b) Olmstead, M. M.; Power, P. P. *J. Am. Chem. Soc.* **1986**, *108*, 4235.

(12) (a) Agou, T.; Kobayashi, J.; Kawashima, T. *Chem. Eur. J.* **2007**, *13*, 8051. (b) Wakamiya, A.; Mori, K.; Yamaguchi, S. *Angew. Chem., Int. Ed.* **2007**, *46*, 4273. (c) Kano, N.; Furuta, A.; Kanbe, T.; Yoshino, J.; Shibata, Y.; Kawashima, T.; Mizorogi, N.; Nagase, S. *Eur. J. Inorg. Chem.* **2012**, 1584.

(13) The DFT calculations were performed by Gaussian 09 program (SI).

(14) (a) Solé, S.; Gabbai, F. P. *Chem. Commun.* **2004**, 1284. (b) Sundararaman, A.; Venkatasubbaiah, K.; Victor, M.; Zakharov, L. N.; Rheingold, A. L.; Jäkle, F. *J. Am. Chem. Soc.* **2006**, *128*, 16554. (c) Pakkirisamy, T.; Venkatasubbaiah, K.; Kassel, W. S.; Rheingold, A. L.; Jäkle, F. *Organometallics* **2008**, *27*, 3056.

(15) In the structure of  $5\cdot\text{F}^-[\text{K}(\text{cryptand})]^+$ , two crystallographically independent molecules were observed, one of which showed a disorder in the core  $\pi$ -skeleton. Thus, the structural features of  $5\cdot\text{F}^-$  are discussed for the other, non-disordered molecule.

(16) All the crystal structures of triarylborane fluoride complexes registered in the CCDC database were examined for reference.

(17) Toyota, S.; Ōki, M. *Bull. Soc. Chem. Jpn.* **1992**, *65*, 1832.